Journal of Materials and Environmental Sciences
ISSN : 2028-2508
CODEN : JMESCN

J. Mater. Environ. Sci., 2018, Volume 9, Issue 8, Page 2370-2378

http://www.jmaterenvironsci.com

Elaboration and Characterization of Recycled PP/Clay Nanocomposites

K. Zdiri [1], A. Elamri [1] *, M. Hamdaoui [1], O. Harzallah [2], N. Khenoussi [2], J. Brendlé [3]

[1] *ENIM - Unité de Recherche Matériaux et Procédés Textiles, Avenue* Ibn *El* Jazzar, *5019 Monastir, Tunisia.*
[2] *Laboratoire de Physique et Mécanique Textiles EA 4365,11 rue Alfred Werner, 68093 Mulhouse , France.*
[3] *Pôle Matériaux à Porosité Contrôlée, IS2M, CNRS-UMR 7361, 3 rue Alfred Werner, 68093 Mulhouse, France.*

Received 17 Nov 2017,
Revised 04 Apr 2018,
Accepted 05 Apr 2018

Keywords

- ✓ *Recycled PP,*
- ✓ Clay,
- ✓ Nanocomposites,
- ✓ Morphology,
- ✓ Rheological.

amri.adel2201 @gmail.com;

Abstract

In this paper, the elaboration and characterization of recycled polypropylene/Tunisian clay nanocomposites has been investigated. When recycled, polypropylene polymer is degraded and has poorer mechanical and rheological properties. To overcome this problem, we proposed to incorporate Tunisian clay nanoparticles in recycled polypropylene (rPP) matrix. The incorporation of Tunisian clay was performed in molten state using maleic anhydride grafted polypropylene (PP-g-MA) as compatibilizer. The dispersion of clay in rPP polymer was evaluated by scanning electron microscopy and Fourier transformed infrared spectroscopy. Thus, Tunisian clay was more dispersed in nanocomposites with the increase of Tunisian clay loading. In dead, the incorporation of silicate layers gave rise to a considerable increase of the static viscosity demonstrating the reinforcing effect of Tunisian clay nanofillers on rPP matrix. However, the increasing trend of morphological and rheological properties is lower when the clay content exceeds 5%.

1. Introduction

Polypropylene (PP) is one of the most versatile and extensively used polymers in the world. Its unique properties and ability to adapt to various fabrication techniques make it stand out as an invaluable material for a wide range of uses [1]. PP is widely used in several applications such as automotive components, aerospace, laboratory equipment, plastic parts, food packaging, geotextiles, and containers [2]. Due to the dramatical increase of polypropylene consumption, each year millions of tons of waste PP are released into the environment [3]. Recycling is an ecofriendly method for the treatment of PP waste and a good opportunity for reducing the environmental impact. The importance lies in the fact that PP recycling process reduces the amount of waste going to landfills, and also because it permits a reduction in the consumption of virgin PP and resources used to produce original polymers. Moreover, recycled PP could be used as an input in the cycle production of new products [4-5].

Nevertheless, the performance of PP polymer is proved to be insufficient during its re-use, particularly with regard to thermo-mechanical properties [6]. The incorporation of nanoparticules as fillers in polymer matrix seems to be one of the most successful solutions to upgrade PP properties [7-8]. The most commonly used nanofillers are montmorillonite, carbon nanofibers, polyhedral oligomeric silsesquioxane, carbon nanotubes, nanosilica, nanoaluminum oxide and nanotitanium oxide [9-10].

Generally clay show poor compatibility with the PP matrix due to the polarity difference between hydrophilic natural filler and hydrophobic polymer. This incompatibility leads to a loss of the properties of the obtained PP/Clay blend [11]. Therefore, the use of a compatibilizer improves the compatibility between clay and the matrix polymer. Anhydride maleic grafted polypropylene (PP-g-MA) is the most common used compatibilizer [12].

The aim of this work is to improve the morphological, physical and rheological properties of rPP, using Tunisian clay as a nanometrical reinforcement. Throughout the study, the dispersion characteristics of clay nanafillers in rPP were evaluated. Rheological characterization, in molten state, of synthetized nanocomposites was evaluated to assess the nanoscale dispersion state.

2. Materials and methods

Recycled PP polymer used in this study is obtained from woven bags used for food packaging. Woven bags are cleaned, washed and dried. Then, the rPP was converted into powders using an MFI-MVI 3350 machine and a chisel. Virgin polymer (vPP), initially used in the manufacture of woven bags, was purchased from SABIC®PP and compared to recycled PP in this study. The clay investigated in present work was smectitic clay obtained from sit of Coniacian-Santonian outcroppings of Jebel Meloussi (Sidi Bouzid region). PP-g-MA, used as compatibilizing agent, was purchased from Sigma-Aldrich, France.

Uncompatibilized recycled PP/clay nanocomposites (UrPPCN) and compatibilized (CrPPCN) ones were prepared by melt mixing using a twin-screw extruder (SIKRC, Nissei Plastic Industrial Co). The compositions of prepared samples are described in Table 1.

Table 1: Compositions of prepared nanocomposites

Sample	Clay (%)	PP-g-MA (%)	Recycled PP (%)
rPP	-	-	100
UrPPCN1	1	-	99
UrPPCN3	3	-	97
UrPPCN5	5	-	95
UrPPCN7	7	-	93
CrPPCN1	1	3	96
CrPPCN3	3	9	88
CrPPCN5	5	15	80
CrPPCN7	7	21	72

Fourier-transform infrared FTIR was used to investigate the structural changes of Tunisian clay, rPP and rPP/clay nanocomposites. The IR spectra were recorded using a Perkin-Elmer model (783) spectrometer.

Thermal analysis was performed using differential calorimeter apparatus TG-DTA 92 SETARAM with a heating rate of 10°C/min. The TG and derivative thermogravimetry (DTG) curves were recorded from 25 to 1000 °C. Differential scanning calorimeter DSC (Perkin Elmer DSC-7) was used for recording DSC scans of the rPP as well as vPP.

Tensile testing of PP polymers was carried out using the Universal Tensile Testing machine equipped with an extensometer, according to the ASTM D638 standard test method at crosshead speed of 5 mm/min at a temperature of 25°C. From the stress-strain curves, Young's Modulus, tensile stress at yield, tensile strength and percent elongation at break values were calculated.

Scanning electron microscopy (SEM) analysis was performed on a JEOL-JSM 5600 LV microscope, equipped with a 6587 EDS (energy dispersive X-Ray spectrometry) detector. It was employed to examine the morphology and fracture surface of Tunisian clay nanoparticles, UrPPCN and CrPPCN nanocomposites.

Rheological behavior was measured with strain-controlled rotational rheometer. Static and dynamic rheological tests were carried out at a constant temperature of 180°C under a nitrogen environment using parallel plate geometry with 25 mm diameter and 1 mm gap.

3. Results and discussion

3.1. PP polymers characterization

Chemical structure

Figure 1 demonstrates that all the peaks of recycled and virgin PP are related to C–H bonds. The absorption peak at wave number 1377 cm^{-1} and 1166 cm^{-1} is attributed to bending and wagging absorption for C–H and C–C stretching characteristic absorption [13]. Indeed, the peak at 808 cm^{-1} originates out of plane C–H bending vibration [14]. For recycled PP, the peaks observed at 712, 873 and 1418 cm^{-1}, which are absent for vPP, correspond to the in and out-plane bending and asymmetrical stretching vibration peaks of O-C-O, respectively. This indicates the presence of calcium carbonate $CaCO_3$ in rPP structure [15].

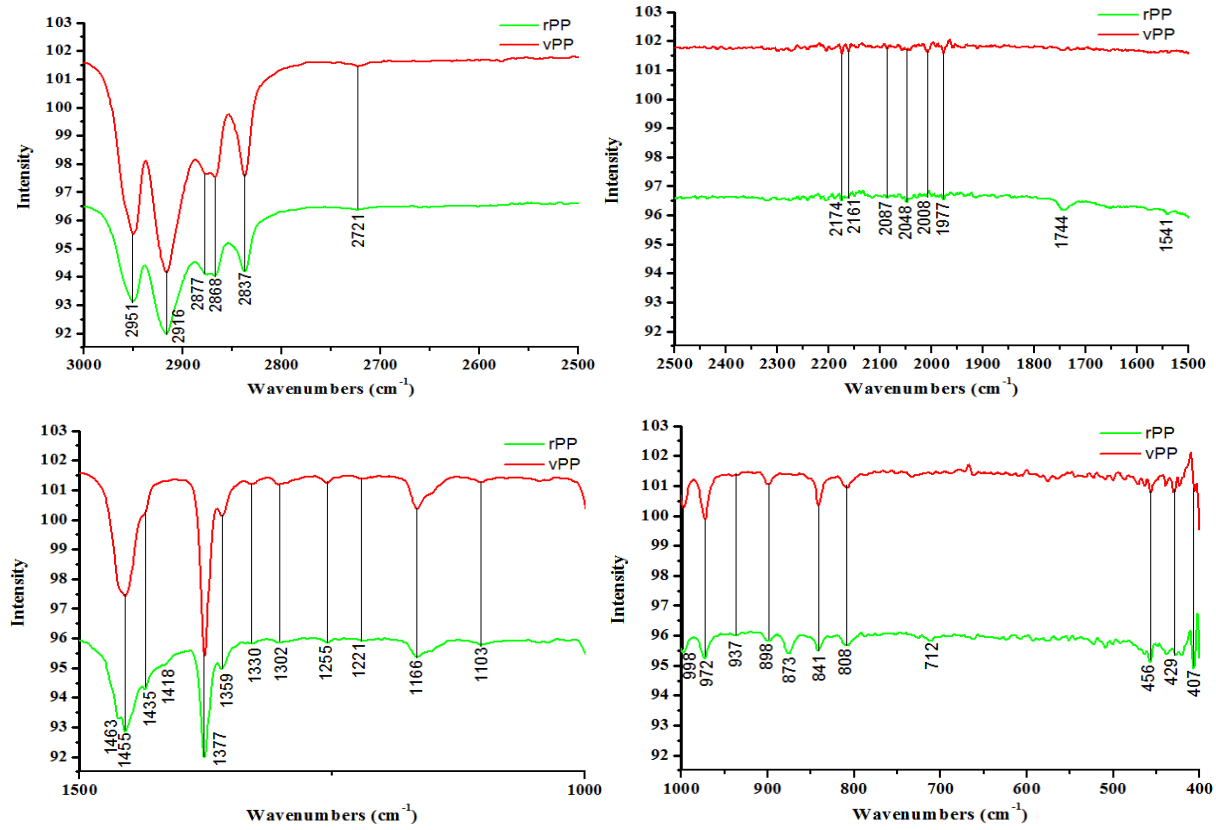

Figure 1. FTIR analysis of recycled and virgin PP polymers

Thermal characteristics

We can see on thermograms of figure 2 that the degradation of vPP starts at the temperature of 260°C while rPP indicated two stages of degradation. The first stage accruing at 245°C belongs to degradation of stearic acid, and the second stage at 600°C corresponds to the decomposition of $CaCO_3$. Moreover, it is clear from DTA diagram that the amount of the released heat from vPP is higher than rPP. This can be explained by the degradation of PP polymer during the recycling process.

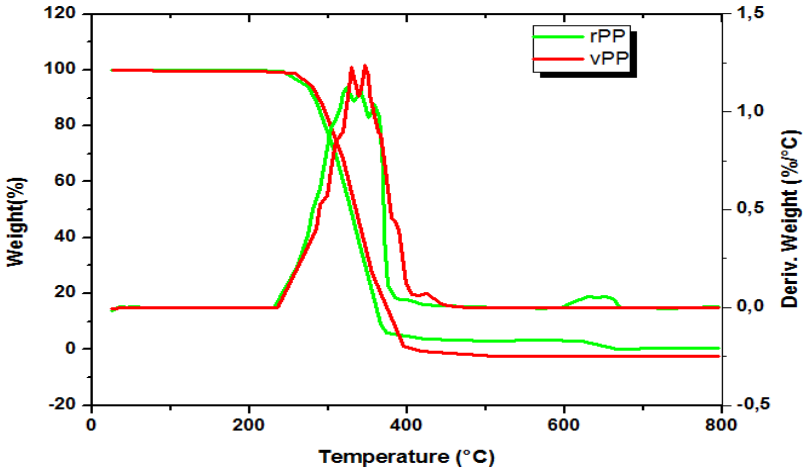

Figure 2. TGA/DTA analysis of rPP and vPP polymers

Thermal properties for rPP and vPP samples are summarized on Table 2:

Table 2: Thermal characteristics of rPP and vPP

Polymer	Tc (°C)	Tm (°C)	ΔHc (J/g)	ΔHm (J/g)	Xc (%)
rPP	116.57	167.02	93.44	82.7	39.56
vPP	104.4	151.73	80.14	56.49	27.028

DSC heating runs on figure 3, revealed two endothermic peaks at 167 °C and 151.73 °C corresponding to melting temperatures of rPP and vPP, respectively. Cooling thermograms are characterized by the presence of crystallization peaks at 116.57 and 104.4 °C. The melting and crystallization peaks of rPP are located at higher temperatures than for vPP. Also, we can observe that both melting enthalpy and crystallization increase, corresponding to an increase in the degree of crystal during recycling process [16]. The shorter polymer chains can form crystals more easily; therefore, crystallinity is increased in rPP which is evident from the brittle fracture in the sample [17]. In fact, lower molecular weight allows chains to fold and build more and more crystal structure [18].

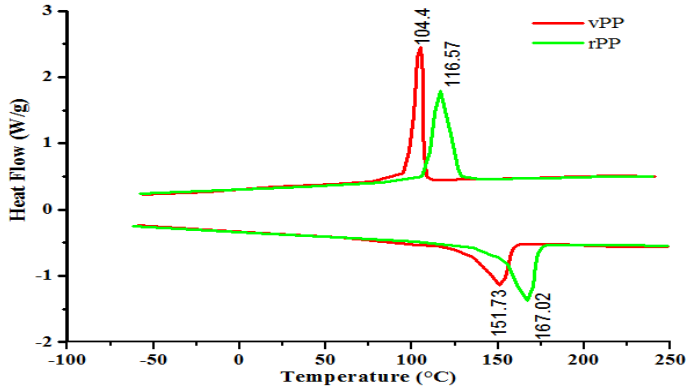

Figure 3. DSC thermograms of recycled and virgin PP polymers

Mechanical properties

Typical stress strain curves of rPP and vPP used in this study are illustrated on Figure 4. Both PP polymers exhibit regions of elastic yielding, and plastic deformation accompanied by cold drawing. One may note that vPP and rPP samples have similar elastic and yield domains but a reduction of the drawing behavior. This can be explained by the higher crystal content of recycled samples and to the reduction of the molecular weight after recycling process [19]. Young's Modulus, stress at yield, tensile strength and strain at break values of rPP were 804.59 MPa, 30 MPa, 35.92 MPa and 609%, respectively. According to Aurrekoetxa [20], lower molecular weight inserts more chain ends into the structure, resulting in fewer chains completely integrated into the crystal to sustain stress during tensile loading, causing failure at lower elongation.

In fact, an increased crystallinity could be caused by the changes in molecular weight, which occurred as a result of polymer degradation during recycling, leading to chain breaking and eventual secondary crystallization [21].This structural modification leads to an increase in its Young's modulus and a decrease in the breaking strain.

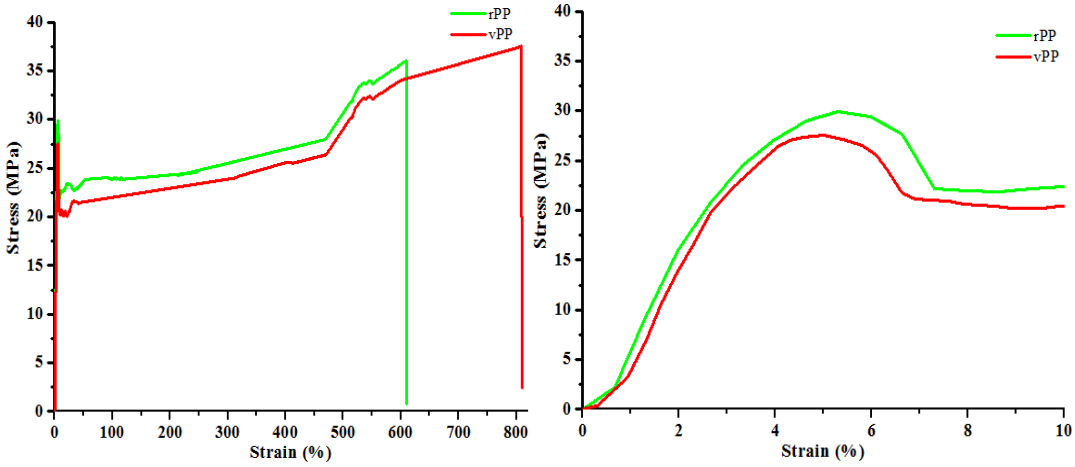

Figure 4. Stress-strain curves of recycled and virgin PP polymers

Rheological behavior

As illustrated on figure 5, virgin PP polymer has a higher Newtonian viscosity than the recycled one. This can be explained by its higher macromolecular weight Mw [22]. It is evident that the chains breakings happen during the recycling process increase the density of short polymer chains that lowers the viscosity.

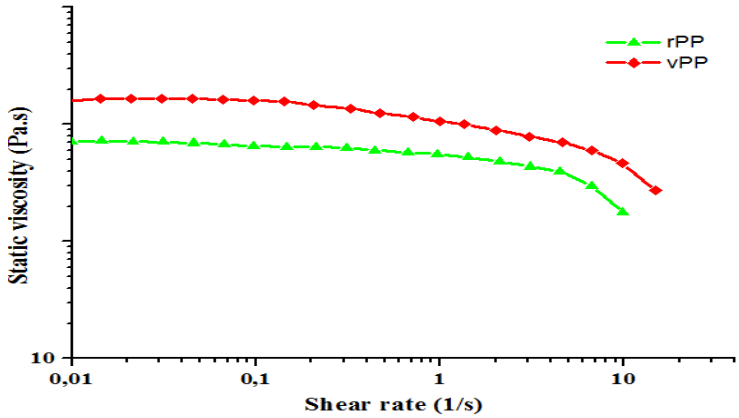

Figure 5. Static viscosity of recycled and virgin polypropylenes

From dynamic rheological tests (figure 6), we observed that there are two different behaviors according to the frequency domain. At high frequency (low relaxation time) the vPP storage modulus (G') is higher than those of rPP. This can be explained by the high viscosity of the vPP and by the higher mobility of the polymer chains. But at low frequencies (long relaxation time) the vPP modulus is less than that of rPP one [23].

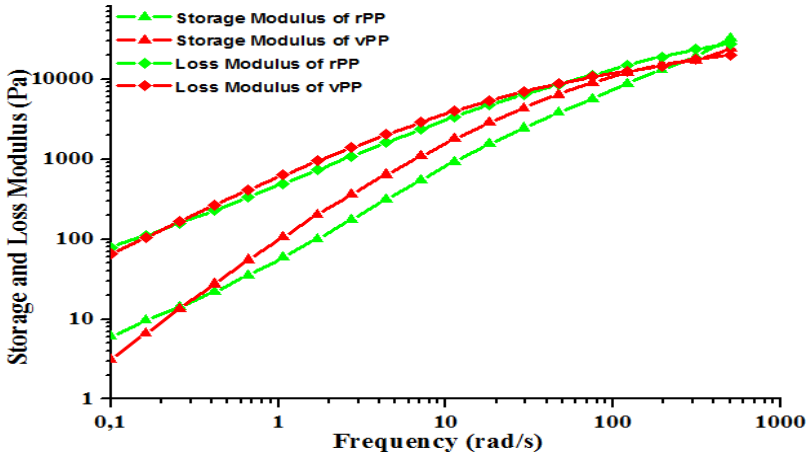

Figure 6. Storage (G') and loss (G'') modulus of virgin and recycled PP polymers

In conclusion, we can say that after recycling process the structure of polypropylene is degraded, causing poorer properties than those of vPP. To overcome these problems, we proposed the addition of nanofiller as Tunisian clay.

3.2. Dispersion of Tunisian clay in CrPPCNs and UrPPCNs

SEM analysis

The phase morphologies of CrPPCN and UrPPCN nanocomposites are represented on figure 7. The dark areas represent an individual Tunisian clay layers or agglomerates while the gray part represents the polypropylene matrix. It is evident from the SEM photograph of UrPPCN (Fig. 7 a, b, c and d) that there were many aggregate of nanoparticles of the order of micrometer level. This proves that tactoids have not been delaminated during mixing, confirming the less chemical interaction between the polar hydroxyl groups on the surface of the clay platelets and the nonpolar polypropylene chains. In contrast, the large aggregates disappeared with the presence of PP-g-MA (Fig. 7 e, f, g and h). The clay particle is finely dispersed within the rPP matrix more uniformly [24, 25]. Comparing Fig. 7 (e), (f), (g) and (h), it was observed that the state of dispersion was enhanced and particles were dispersed more uniformly as the percentage of compatibilizer and organoclay was increased [26]. These results could be attributed to enhanced interfacial adhesion due to the increased amount of PP-g-MA and also to the well dispersion of organoclay layers inhibiting possible coagulation of the dispersed phase. In fact, the addition of PP-g-MA facilitates the expansion of the interlayer space of reinforcing nanolayers by intercalating of certain polar groups between the silicate layers through hydrogen bonding to the oxygen groups of the silicate tetrahedral. This makes it possible to separate and disperse clay layer in a homogeneous manner. The best dispersion among all nanocomposites is observed in the nanocomposite containing 5 wt% organoclay.

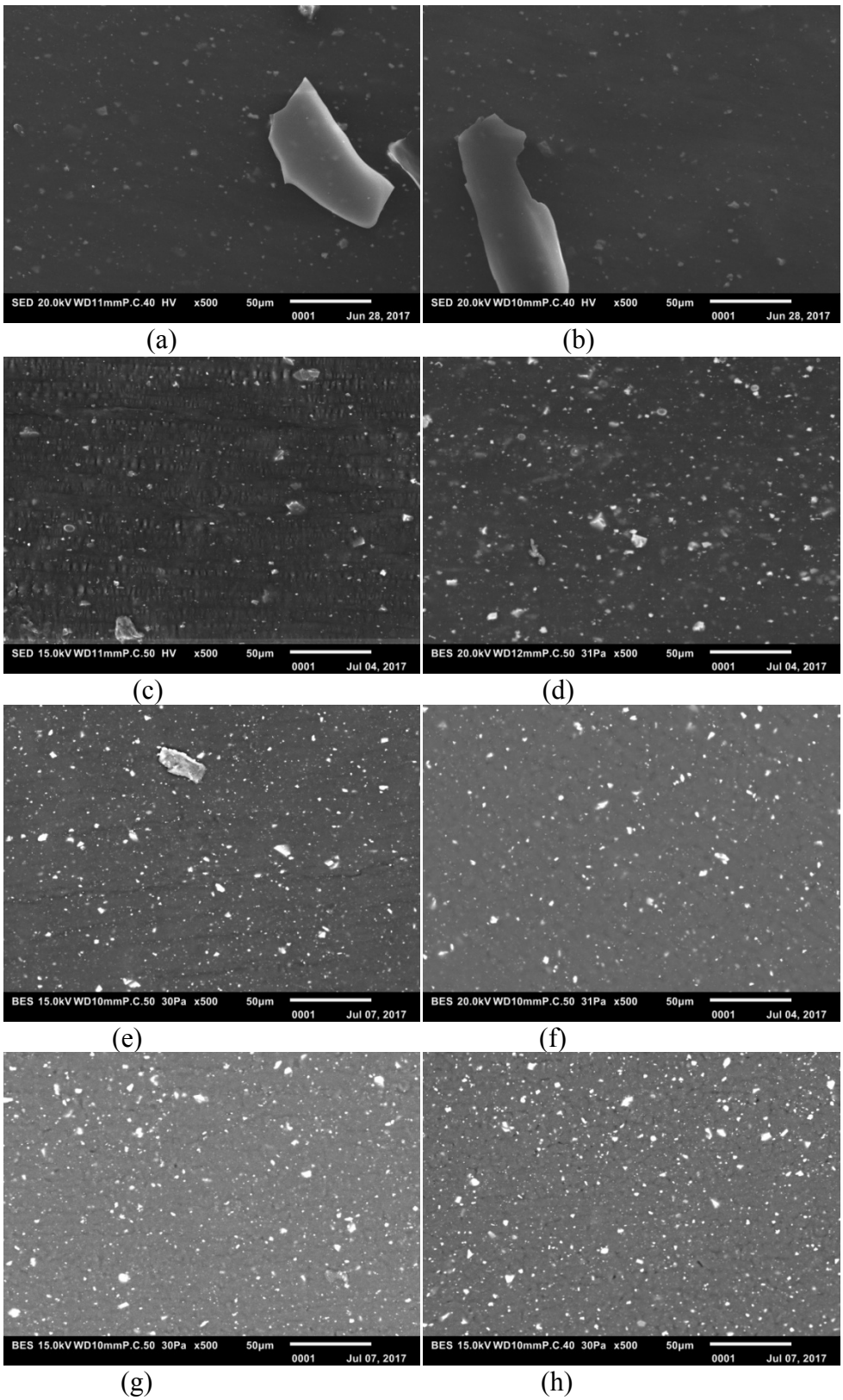

Figure7. SEM micrographs of nanocomposites :
(a): UrPPCN1. (b): UrPPCN3. (c): UrPPCC5. (d) : UrPPCN7
(e): CrPPCN1. (f): CrPPCN3. (g): CrPPCN5. (h): CrPPCN7

Chemical analysis

FTIR spectra of rPP, organoclay, UrPPCN and CrPPCN are presented on figure 8. The results of the IR spectra of Tunisian organoclay confirmed the presenceof illite and kaolinite at 3696 and 3627 cm^{-1}, respectively. Other vibrations at 912.1, 796, 779.10 and 693 cm^{-1} are also characteristics of silicate minerals. The main non clay

mineral was quartz detected by the band at 420 cm^{-1} [27]. Tunisian clay nanoparticules alter the shape of observation band of PP between 1163-400 cm^{-1} and 3000-2800 cm^{-1} corresponding interaction between nanoclay and rPP. In the rPP/clay nanocomposites, the characteristics vibrations of Tunisian clay are present in addition to the features from rPP centered at 420, 471, 527, 693, 693, 796, 912, 1004, 1026, 1100, 1163, 2850 and 2920 cm^{-1} [28]. The observation band at 1026 and 1100 cm^{-1} related to the interaction between nanoclay and recycled polymer is enhanced by hydrogen bonding between COOH groups and oxygen groups of silicate. A slight increase in an intensity of the band with an increase of nanoclay content in rPP/clay with and without compatibilizer was observed compared to neat rPP. Indeed, the intensity of band in CrPPCN with compatibilizer (Figure 8 d, e and f) is higher compared to those of UrPPCN without compatibilizer (Figure 8 a, b, c). Also, the bands observed at 420, 471 and 527 cm^{-1} are very clear in the compatibilized system compared to those of uncompatibilized system. These observations can be explained by the low chemical interactions between polymer and nanofiller took place in the incompatibilized system.

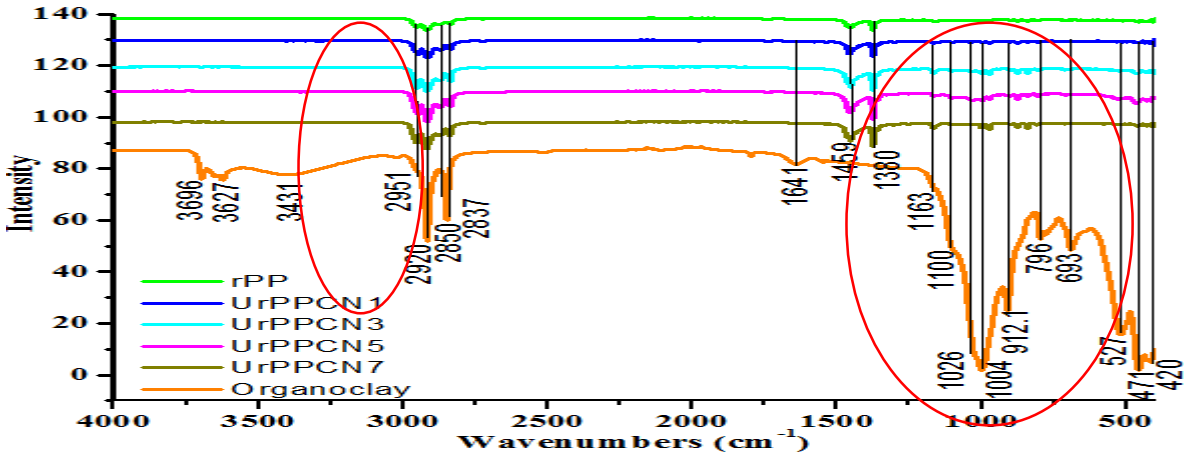

(a)

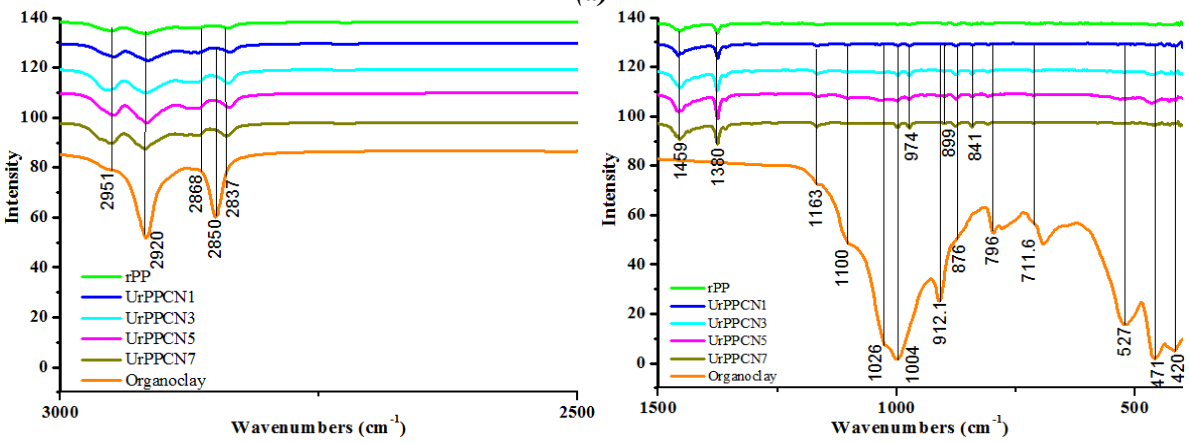

(b) *(c)*

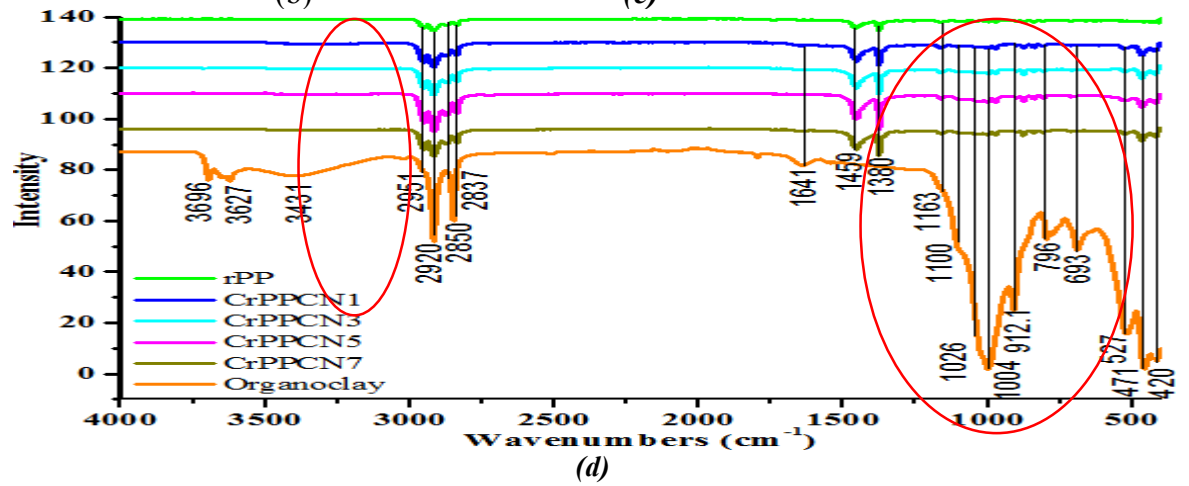

(d)

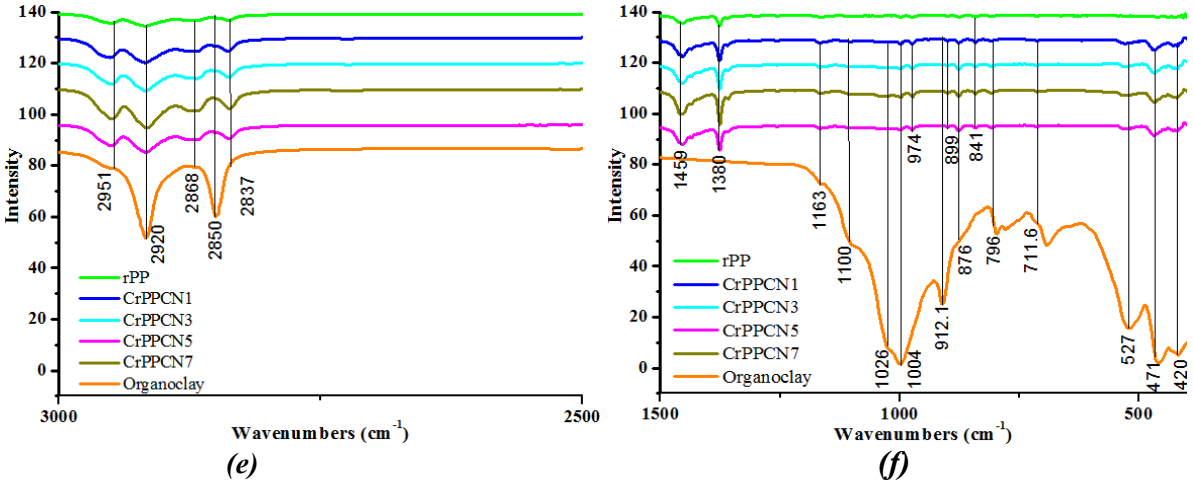

Figure 8. FTIR spectra of (a, b, c) UrPPCNs and (d, e, f) CrPPCNs nanocomposites

Melt rheological behavior

Dynamic flow curves of pristine rPP, UrPPCN and CrPPCN nanocomposites are reported on figure 9. At low angular frequencies, we can observe a very large increase in the viscosity of the nanocomposites compared to that of neat rPP. This increase is much higher for the compatibilised nanocomposite samples CrPPCN. This could result from the strong interactions between the organoclay, the polymer matrix and the compatibiliser. Indeed, the complex viscosity of CrPPCN5 is 3226 Pa.s at 0.01 Hz, whereas it is 1659 Pa.s for UrPPCN5 and only 719 Pa s for the neat rPP. In addition, augmentation of the Tunisian organoclay content induces a sharp increase of static viscosity, especially in the low angular frequency regime. The results indicate that the incorporation of Tunisian clay into the rPP matrix has good reinforcing effect. For both compatibilized and uncompatibilized nanocomposites, a clear increase of static viscosity is obtained in the case of 5 wt % of Tunisian organoclay.With further increase in nanoclay loading from at 7 wt%, a decrease of the viscosities of nanocomposites was observed [29].

Moreover, the viscosity of CrPPCN5 is 3226 Pa.s at 0.05 Hz, whereas it is 2556 Pa.s for CrPPCN7 and only 719 Pa.s for neat rPP. One possible reason for this kind of behaviour may be attributed to the low chemical interaction, thereby reducing the contact surface area between the organoclay and the rPP matrix.

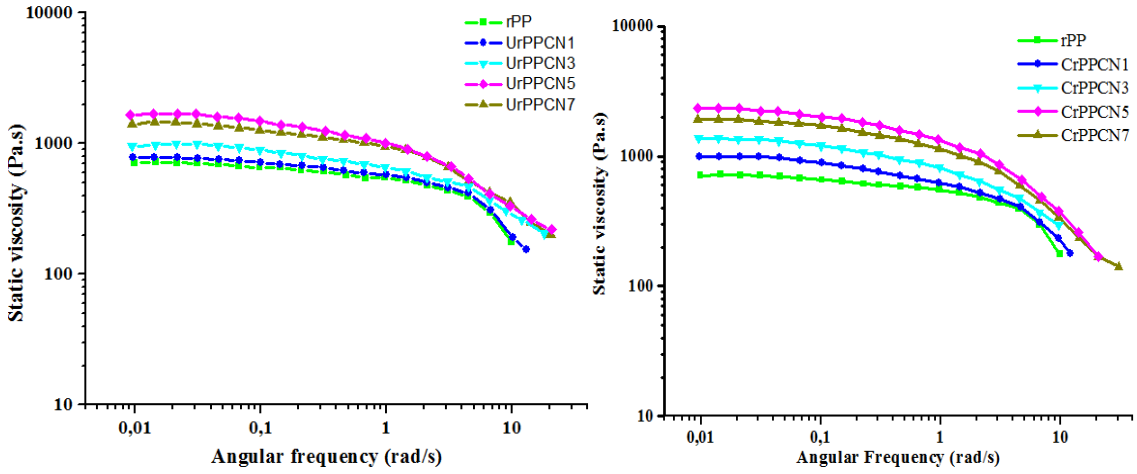

Figure 9. Effect of nanoclay on dynamic viscosity of rPP, UrPPCN and CrPPCN

4. Conclusion

The structure and properties of the recycled PP are degraded causing poorer properties after recycling process. The mechanical and dynamical properties (G', G" and η*) of rPP are lower than those of vPP. Crystallization temperature of rPP increases following a decrease of the crystallization temperature. In the case of rPP polymer blends issued from recycling, we can improve properties by addition of reinforcements such as Tunisian clay which will enhance its performance.

The effects of concentrations of organoclays and compatibilizers on the morphology, structural and rheological properties of rPP were investigated. The incorporation of the nanoclay in the presence of PP-g-MA, taken as compatibilizer, significantly improves the morphological and rheological properties of the rPP at a good level. It

became apparent that PP-g-MA intercalated between silicate layers of Tunisian clay and therefore improved the dispersibility of the clay nanoparticle in the CrPPCN. Also, the static viscosity and the intensity of band in compatibilized samples are higher compared to those of UrPPC, which could result from the strong interactions between the organoclay, the polymer matrix and the compatibiliser.

The structural and rheological properties of CrPPCN could be significantly improved by the incorporation of Tunisian clay; the static viscosity of rPP/clay nanocomposites was higher than that of pristine rPP. This increase in properties with clay loading can be explained by the effect reinforcement of clay nanofiller.

Finally, the best improvement in morphological, structural and rheological properties were obtained for the nanocomposites containing 5 wt% Tunisian clay and 15 wt% PP-g-MA.The effect observed can be explained by the less bonding between rPP matrix and clay at higher clay loading.

References

1. H. A. Maddah, *American Journal of Polymer Science*, 6 (2016) 1-11.
2. J. Jarugala, J. PreshdReddy, R. Kasilingam, M. Nawale, S. Sahoo, E. R. Sadiku, *Int. J. Adv. Res.,* 5 (2016) 1021-1028.
3. K. Zdiri, A. Elamri, M. Hamdaoui. *Polym. Plast. Technol. Eng.* 56 (2017) 824–840.
4. N.S. Suharty, B. Wirjosentono, M. Firdaus, D.S. Handayani, J. Sholikhah, Y.A. Maharani, *Int. J. Phys. Sci.*, 19 (2008) 105–115.
5. M. Sain, J. Balatinecz, S. Law, *J. Appl. Polym. Sci.,* 77 (2000) 260.
6. M. Zanetti, S. Lomakin, and G. Camino, *Macromol. Mater. Eng.*, 279 (2000) 1–9.
7. M. R. Abadchi, A. Jalali-Arani, *Thermochimica Acta*, 617 (2015) 120-128.
8. D.G. Dikobe, A.S. Luyt, *Thermochimica Acta*, 654 (2017) 40-50.
9. H. Nafchi, M. Abdouss, S. Najafi, R. Gargari, M. Mazhar, *Maderas-Cienc. Tecnol.,* 17 (2015) 45-54.
10. K. S. Chun, S. Husseinsyah, and F. N. Azizi, *Polym. Plast. Technol. Eng.*, 52 (2013) 287–294.
11. M. Claudia, C. Bonelli, A. F. Martins, E. B. Mano, C. L. Beatty, *Journal of Applied Polymer Science*, 80 (2001) 1305–1311.
12. M. Ataeefard, S. Moradian, *Polym. Plast. Technol. Eng.,* 50 (2011) 732–739.
13. B. J. Luijsterburg, *Mechanical recycling of plastic packaging waste Eindhoven*: Technische Universiteit Eindhoven (2015).
14. M. R. Husin, A. Arsad, S. S. Suradi, O. Alothman, N. Ngadi, M. J. Kamaruddin, *Chemical Engineering Transactions, Italian Association of Chemical Engineering* , 56 (2017) 1015-1020.
15. S. Abdolmohammadi, S. Siyamak, N. Ibrahim, W. Yunus, M. Zaki Ab Rahman, S. Azizi and A. Fatehi. *Int. J. Mol. Sci.* 13 (2012) 4508-4522.
16. J. Arkan Hadi, G. Faisal Najmuldeen and K. Yusoh, *J. Polym. Eng.*, 33 (5) (2013) 471–481.
17. I. Goitisolo, J.I. Eguiazábal, J. Nazábal, *Polym. Degrad. Stabil.*, 93 (2008) 1747–1752.
18. N. Touati, M. Kaci, S. Bruzaud, Y. Grohens, *Polym. Degrad. Stabil.*, 96 (2011) 1064–1073.
19. L. Chocinski-Arnault, F. Touchard, M. Comyn, M. Taha, M.P. Buron, *Journées Nationales sur les Composites*, France (2011) 52.
20. J. AURREKOETXEA, *J. Mater. Sci.*, 36 (2001) 2607 – 2613.
21. J. S. Fabiyi, A. G. McDonald, *Maderas*, *Ciencia y Tecnologia,* 16 (3) (2014) 275-290.
22. A. Elloumi, S. Pimbert, A. Bourmaud, C. Bradai, *Polym. Eng. Sci.*, (2010) 1905-1911.
23. N. T. Phuyong, V. Gilbert, *J. Reinf. Plast. Comp.,* 27 (2008) 1983-2000.
24. F. Lei, Y. HN, S. Yang, H. Sun, J. Li, S. Guo, H. Wu, JB. Shen, R. Chen, Y. Xiong. *Polym.*, 82 (2016) 274-284
25. Y. Dong, D. Bhattacharyya, *Composites: Part A*. 39 (2008) 1177–1191.
26. H. M. Gabr, W. Okumura, H. Ueda, W. Kuriyama, K. Uzawa, I. Kimpara, *Composites: Part B.* 69 (2015) 94–100.
27. J.E. Boulingui, C. Nkoumbou, D. Njoya , F. Thomas, J. Yvon, *Appl. Clay Sci.,* 115 (2015) 132–144.
28. C.K. Hong, M.J. Kim, S.H. Oh, Y.S. Lee, C. Nah, *J. Ind. Eng. Chem.,* 14 (2008) 236–242.
29. T. Naima, K. Mustapha, B. Stephane, G. Yves, *Polym. Degrad. Stabil.* 96 (2011)1064-1073.